IEEE Access
Multidisciplinary | Rapid Review | Open Access Journal

Received June 9, 2018, accepted July 3, 2018, date of publication July 11, 2018, date of current version August 7, 2018.

Digital Object Identifier 10.1109/ACCESS.2018.2854774

Performance Analysis of Cooperative Relaying Systems With Power-Domain Non-Orthogonal Multiple Access

YINGYING ZHANG[1], ZHEN YANG[1], YOUHONG FENG[1,2], (Student Member, IEEE), AND SHIHAO YAN[3], (Member, IEEE)

[1]Key Laboratory of Ministry of Education in Broadband Wireless Communication and Sensor Network Technology, Nanjing University of Posts and Telecommunications, Nanjing 210003, China
[2]College of Physics and Electronic information Engineering, Anhui Normal University, Wuhu 241000, China
[3]School of Engineering, Macquarie University, Sydney, NSW 2109, Australia

Corresponding author: Zhen Yang (yangz@njupt.edu.cn)

This work was supported in part by the National Natural Science Foundation of China under Grant 61671252 and in part by the Innovation Program of Graduate Education of Jiangsu Province, China, under Grant KYLX150833.

ABSTRACT Non-orthogonal multiple access (NOMA) is one of the promising radio access techniques in 5G communication networks. In this paper, a cooperative NOMA relaying scheme with two-phase superposition coding is proposed to enhance the performance of NOMA relaying systems. In the proposed scheme, the source simultaneously transmits two symbols using superposition coding in the first time slot, while the relay decodes the symbols by employing the successive interference cancellation. In the second time slot, the relay forwards the two symbols with a new superposition coding to the destination, which jointly decodes them by employing maximum-ratio combining technology over the received signals from both the source and relay. In order to reveal the benefits of the proposed scheme, its achieved ergodic sum rate, outage probability, and throughput are analyzed with imperfect channel state information taken into account. Our examination shows that the proposed scheme can significantly outperform existing schemes in terms of achieving a higher ergodic sum rate, a lower outage probability, or higher throughput at the cost of a slightly increased complexity.

INDEX TERMS Non-orthogonal multiple access (NOMA), power allocation, relay network, sum rate.

I. INTRODUCTION

Wireless communications are becoming ubiquitous in our daily life due to the increasing number of smart devices and related applications, which leads to the ever-increasing demand for massive wireless connections and large amounts of data traffic [1]. The emerging non-orthogonal multiple access (NOMA) technique has the ability to guarantee these requirements. Thus, NOMA is considered to be a key technique and research focus for the next generation communications, which benefit from the superior spectral efficiency and high rate of NOMA [2]–[5]. NOMA generally can be divided into two categories, namely power-domain NOMA (PD-NOMA) [6] and code-domain NOMA, including sparse code multiple access (SCMA) [7]. In a PD-NOMA system, the transmitter side allows multiple users to share the same time, code or frequency resource simultaneously, but with different power levels. For a SCMA system, the signal of each user is transmit with various codebooks. At the receiver side of NOMA systems, the successive interference cancellation (SIC) will be employed to decode the desired signals sequentially [8]. For SCMA, the message passing approach (MPA) is applied to detect the signal of each user [9]. Moltafet *et al.* [10] compared the SCMA with PD-NOMA system and their results showed that the SCMA can achieve a higher sum rate than the PD-NOMA at the cost of a higher system complexity. Furthermore, a new approach of cellular networks called power domain sparse code multiple access (PSMA) is proposed in [11], where the power domain and the code domain are both adopted to transmit multiple users' signals over a subcarrier simultaneously, and as shown the PSMA gains better spectral efficiency at the cost of an increase in the system complexity. Considering the low system complexity, we focus on power-domain NOMA in this paper. Henceforth, this paper refers to

PD-NOMA simply by NOMA. In [12], the performance in terms of the outage probability and achievable sum-rate for a particular user of NOMA scheme was discussed. The system-level performance was discussed for NOMA scheme in [13], which shows that NOMA can achieve a remarkable gain over the orthogonal multiple access (OMA) scheme. It should be noted that the perfect SIC is only considered in this paper.

The joint application of cooperative relay and NOMA has recently attracted growing interests to further enhance the performance of NOMA systems [14]– [16]. The key idea of NOMA is to allocate more power to the users with low channel qualities, however, the performance improvement brought by NOMA is relatively constrained. In cooperative communications, the source transmits information to the desired destinations with the assistance of several relays, which can further improve the system performance. In [17], the outage and throughput performance of cooperative NOMA systems was investigated, where user near to the source works as a half-duplex (HD) and full-duplex (FD) relay using decode-and-forward (DF) strategy to improve the performance of the far user. To be more specific, a cooperative communication scheme with NOMA was introduced in [18], in which the users with high channel qualities can serve as relays to improve the communication between the users with poor channel conditions and the base station (BS). Furthermore, in order to improve the communication reliability for users with poor channel conditions, a cooperative NOMA transmission scheme with a dedicated relay was introduced in [19]. Liu *et al.* [20] introduced a collaborative NOMA assisted relaying system, where three users were served by BS, and the user nearest to the BS was served as a relay to establish the communication between BS and the other two users. To improve the performance of the cell-edge user, [21] proposed two cooperative relaying schemes, where an on/off mechanism was proposed to decide whether the FD/HD relaying transmission is necessary or not, respectively. Zhang *et al.* [22] examined the performance of downlink cooperative NOMA system with FD relaying, where the near user acts as a FD relay to help the far user communicating with BS and the optimal power allocation was considered by taking the fairness between the near user and far user into account. Mohammadi *et al.* [23] analyzed the throughput of a full-duplex DF system, where the time-switching protocol was applied by using multi-antenna relays. Besides, [24]– [26] studied the relay selection (RS) strategy for multi-relay NOMA networks. In particular, Ding *et al.* [24] proposed a two-stage RS strategy and the analytical results demonstrated that this strategy can achieve the minimal outage probability and maximal diversity gain. In [25], Deng *et al.* investigated the joint user and relay selection algorithm for the cooperative NOMA system, where multiple users transmit information to two destination with the help of multiple amplify-and-forward (AF) relays. In addition, an optimal selection strategy was proposed at the user-relay pairs in [25]. The work in [26] proposed two optimal RS schemes for the cooperative NOMA with fixed and adaptive power allocations at the relays, respectively. In [27], the accurate and asymptotic expressions of the achievable sum rate for the cooperative communication relaying systems with NOMA (CRS-NOMA) scheme were presented. In [28], a novel CRS-NOMA (NCRS-NOMA) scheme was introduced, where a new detection scheme with maximum-ratio combination (MRC) was discussed, which gains better system performance than the one in [27]. However, since the MRC in [28] requires the symbol which allocated with lower power in the first time slot to be decoded first [29] in the second time slot, and the symbol with higher power can be only acquired from the source to destination link that suffers from the worse channel condition, the performance of this system is limited.

In this paper, we propose a cooperative NOMA relaying system with two-phase superposition coding (CONOMA-TPSC) scheme. Different from the existing works in [27] and [28], where the relay only forwards one symbol, the relay is allowed to simultaneously transmit two symbols by using new power allocation coefficients in our proposed scheme. Moreover, the destination will conserve the signal received from the source instead of decode it until it receives the signal from the relay, and then the destination decodes the symbols received from the source and relay jointly by involving the MRC and SIC. In our proposed scheme, the destination can obtain both the two symbols through the relay to destination link, enables our scheme to achieve higher performance over the previous works. Furthermore, we analyze the ergodic sum rate, and outage probability for our proposed CONOMA-TPSC scheme by considering the imperfect channel state information (CSI), which has not been taking into account in the performance analysis of [27] and [28]. In addition, we also investigate the system throughput for the CONOMA-TPSC scheme. The system throughput is denoted as the product of the fixed transmission rate of users and the communication probability, which is meaningful to quantify the average amount of the successfully transmitted information [30], [31]. And simulation results demonstrate that our proposed scheme achieves a remarkable gain over the NCRS-NOMA and CRS-NOMA schemes proposed in [27] and [28], especially when the transmit power of the source is high.

The remainder paper is organized as follows: Section II presents the system model of our proposed CONOMA-TPSC scheme. Section III analytically characterizes the ergodic sum rate, outage probability, and throughput performance of our proposed scheme. Then numerical results are discussed in Section IV to verify the theoretical expressions in Section III. Finally, Section V concludes this work and introduces future works.

II. SYSTEM MODEL

As illustrated in Fig. 1, we propose a CRS-NOMA communication system which consists of one source (S), one relay (R), and one destination (D). We clarify that the communication

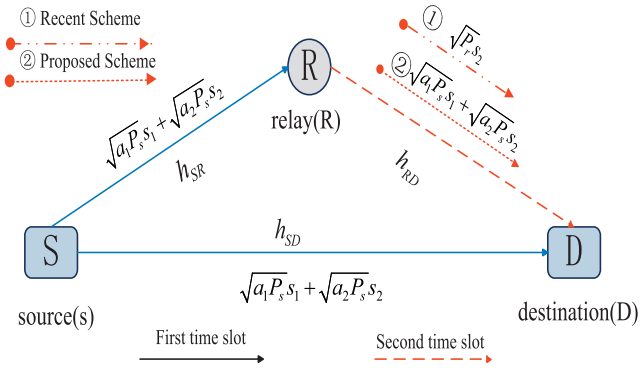

FIGURE 1. System models.

between S and D can be conducted via both the direct link and the relay link, and the relay operates in half-duplex mode using decode-and-forward strategy. We assume that h_{SD}, h_{SR}, and h_{RD} denote the channel coefficients from the source to the destination(S-D), from the source to the relay(S-R), and from the relay to the destination (R-D), respectively, which are subject to Rayleigh fading with variances β_{SD}, β_{SR}, and β_{RD}, respectively.

In practical systems, it is extremely difficult to obtain the perfect CSI of the wireless networks due to the channel estimation errors, which is mainly caused by feedback delay errors [32]. In this work, we assume the estimation of h_i is $\tilde{h}_i$, $i \in \{SR, SD, RD\}$, and the channel coefficients can be modeled as $h_i = \tilde{h}_i + \kappa e_i$, where $e_i \sim \mathcal{CN}(0, {\sigma_{e_i}}^2)$ presents the channel error vector which can be approximated as a Gaussian random variable and κ denotes the impact factor of estimation error. In addition, we can obtain $\tilde{\beta}_i = \beta_i - {\sigma_{e_i}}^2$ by assuming that $\tilde{h}_i$ is statistically dependent of e_i [33].

Each data transmission from the source to the destination takes two time slots. As depicted in Fig. 1, the source transmits two symbols s_1 and s_2 simultaneously to the relay and the destination in the first time slot powers a_1P_s and a_2P_s as the transmit power, respectively, where a_1 and a_2 represent power allocation coefficients with $a_1 + a_2 = 1$ and P_s denotes the transmit power at the source. Thus, the received signals at the relay and the destination during the first time slot are given, respectively

$$y_R = (\tilde{h}_{SR} + \kappa e_{SR})(\sqrt{a_1P_s}s_1 + \sqrt{a_2P_s}s_2) + n_R, \quad (1)$$

$$y_{D_1} = (\tilde{h}_{SD} + \kappa e_{SD})(\sqrt{a_1P_s}s_1 + \sqrt{a_2P_s}s_2) + n_{D_1}, \quad (2)$$

where n_R and n_{D_1} denote additive white Gaussian noise (AWGN) with zero mean and variance σ^2. Without loss of generality, s_1 is allocated with more transmit power, i.e., $a_1 > a_2$. Based on the protocol of NOMA technology, the relay decodes s_1 first by treating s_2 as interference, and then it acquires s_2 through SIC decoding subject to AWGN only. In this manner, the effective (signal-to-noise ratios) SNRs for s_1 and s_2 at the relay can be, respectively, expressed as [33]

$$\gamma_1^R = \frac{\left|\tilde{h}_{SR}\right|^2 a_1P_s}{\left|\tilde{h}_{SR}\right|^2 a_2P_s + \kappa^2\sigma_{e_{SR}}^2P_s + \sigma^2}, \quad (3)$$

$$\gamma_2^R = \frac{\left|\tilde{h}_{SR}\right|^2 a_2P_s}{\kappa^2\sigma_{e_{SR}}^2P_s + \sigma^2}. \quad (4)$$

Meanwhile, the symbol s_1 only can be acquired from the source through the S-D link since the relay forwards symbol s_2 with full power [28]. Hence, the system performance of this protocol is limited. In order to solve this problem, the relay forwards both s_1 and s_2 with a new superposition coding to the destination in our proposed scheme. Therefore, in the second time slot, the received signal at D is given by

$$y_{D_2} = (\tilde{h}_{RD} + \kappa e_{RD})(\sqrt{b_1P_r}s_1 + \sqrt{b_2P_r}s_2) + n_{D_2}, \quad (5)$$

where P_r denotes the transmit power of the relay, n_{D_2} denotes AWGN with zero mean and variance σ^2, b_1 and b_2 represent new power allocation coefficients with the total transmit power constraint $b_1 + b_2 = 1$ and suppose $b_1 > b_2$.

In our proposed scheme, the destination will conserve the received signal y_{D_1} instead of decoding it, and then the MRC is adopted to combine the received signals y_{D_1} and y_{D_2} for decoding purpose at the destination. By employing the MRC technology, the transmitted symbol s_1 is decoded first at the destination, and the symbol s_1 will be subtracted from the received signals y_{D_1} and y_{D_2} with SIC. Then the symbol s_2 will be decoded with another MRC. Define $\tilde{\lambda}_\delta \triangleq \left|\tilde{h}_\delta\right|^2$, $\delta \in \{SR, SD, RD\}$. The corresponding effective SNRs for s_1 and s_2 at the destination are given by

$$\gamma_1^D = \frac{\tilde{\lambda}_{SD}a_1\rho_s}{\tilde{\lambda}_{SD}a_2\rho_s + \psi_{SD,s}} + \frac{\tilde{\lambda}_{RD}b_1\rho_r}{\tilde{\lambda}_{RD}b_2\rho_r + \psi_{RD,r}}, \quad (6)$$

$$\gamma_2^D = \frac{\tilde{\lambda}_{SD}a_2\rho_s}{\psi_{SD,s}} + \frac{\tilde{\lambda}_{RD}b_2\rho_r}{\psi_{RD,r}}, \quad (7)$$

where $\psi_{i,j} = \kappa^2\sigma_{e_i}^2\rho_j + 1$, $i \in \{SR, SD, RD\}$, $j \in \{s, r\}$.

Based on the fact that the end-to-end transmission rate of DF relaying is dominated by the worst link [34], the achievable rates of s_1 and s_2 are given by

$$C_1 = \frac{1}{2}\log_2(1 + \gamma_1), \gamma_1 = \min(\gamma_1^R, \gamma_1^D), \quad (8)$$

$$C_2 = \frac{1}{2}\log_2(1 + \gamma_2), \gamma_2 = \min(\gamma_2^R, \gamma_2^D), \quad (9)$$

where the factor $\frac{1}{2}$ is due to the fact that two time slots are needed to accomplish one round transmission.

III. PERFORMANCE ANALYSIS

In this section, we examine the system performance in terms of the ergodic sum rate, outage probability and system throughput in order to reveal the benefits of our proposed scheme relative to the exisiting schemes in [27] and [28].

A. ERGODIC SUM RATE

Ergodic sum rate is an important performance metric for wireless communication, and thus we now focus on the ergodic achievable rate performance of the proposed system.

The following theorem provides the cumulative distribution function (CDF) of γ_1 for the proposed scheme.

Theorem 1: The closed-form expression for the CDF of γ_1 is given by

$$F_{\gamma_1}(x)=\begin{cases}1-e^{-\left(\frac{\psi_{SR,s}\Omega(x)}{\tilde{\beta}_{SR}}+\frac{\psi_{SD,s}\Omega(\eta)}{\tilde{\beta}_{SD}}\right)}, & 0<x<a_1/a_2,\\ 1, & x\geq a_1/a_2,\end{cases} \tag{10}$$

where $\Omega(\theta)=\frac{\theta}{(a_1-\theta a_2)\rho_s}$, $\theta\in\{\eta,x\}$ and $\eta=x-\frac{b_1}{b_2}$.

Proof: The CDF of γ_1 can be written as follows:

$$F_{\gamma_1}(x)=\Pr\{\gamma_1<x\}=1-\Pr\{\gamma_1>x\}. \tag{11}$$

By definition, $\overline{F}_{\gamma_1}$ denotes the complementary cumulative distribution function (CCDF) of γ_1, the process can be calculated as follows:

$$\begin{aligned}\overline{F}_{\gamma_1}(x)&=\Pr\left\{\min\left(\gamma_1^R,\gamma_1^D\right)>x\right\}\\&=\Pr\{\frac{\tilde{\lambda}_{SR}a_1\rho_s}{\tilde{\lambda}_{SR}a_2\rho_s+\psi_{SR,s}}>x,\frac{\tilde{\lambda}_{SD}a_1\rho_s}{\tilde{\lambda}_{SD}a_2\rho_s+\psi_{SD,s}}\\&\quad+\frac{\tilde{\lambda}_{RD}b_1\rho_r}{\tilde{\lambda}_{RD}b_2\rho_r+\psi_{RD,r}}>x\}.\end{aligned} \tag{12}$$

It is challenging to obtain the exact expression of CCDF directly, so some approximations are made by analyzing the CCDF of γ_1. Using the probability density functions (PDFs) $f_{\tilde{\lambda}_\delta}(x)=\frac{1}{\tilde{\beta}_\delta}e^{-\frac{x}{\tilde{\beta}_\delta}}$ for $\delta\in\{SR,SD,RD\}$, the approximated CCDF of γ_1 is finally obtained as

$$\begin{aligned}&\overline{F}_{\gamma_1}(x)\\&\approx\Pr\{\frac{\tilde{\lambda}_{SR}a_1\rho_s}{\tilde{\lambda}_{SR}a_2\rho_s+\psi_{SR,s}}>x,\frac{\tilde{\lambda}_{SD}a_1\rho_s}{\tilde{\lambda}_{SD}a_2\rho_s+\psi_{SD,s}}+\frac{b_1}{b_2}>x\}\\&\overset{(a)}{=}\Pr\left\{\tilde{\lambda}_{SR}>\frac{\psi_{SR,s}x}{a_1\rho_s-xa_2\rho_s}\right\}\cdot\Pr\left\{\tilde{\lambda}_{SD}>\frac{\psi_{SD,s}\eta}{a_1\rho_s-\eta a_2\rho_s}\right\}\\&=\int_{\psi_{SR,s}\Omega(x)}^{\infty}\frac{1}{\tilde{\beta}_{SR}}e^{-\frac{v}{\tilde{\beta}_{SR}}}dv\cdot\int_{\psi_{SD,s}\Omega(\eta)}^{\infty}\frac{1}{\tilde{\beta}_{SD}}e^{-\frac{u}{\tilde{\beta}_{SD}}}du\\&=e^{-\left(\frac{\psi_{SR,s}\Omega(x)}{\tilde{\beta}_{SR}}+\frac{\psi_{SD,s}\Omega(\eta)}{\tilde{\beta}_{SD}}\right)},\end{aligned} \tag{13}$$

where step (a) relies on $a_1>a_2\,x$. If this condition is not satisfied, we have $\overline{F}_{\gamma_1}(x)=0$. Thus, substituting (13) into (11), (10) can be obtained and the proof is completed. ■

We present the CDF of γ_2 for our proposed scheme in the following theorem.

Theorem 2: The closed-form expression for the CDF of γ_2 is given by

$$F_{\gamma_2}(x)=1-\varphi_1e^{-(\omega_1+\omega_2)x}+\varphi_2e^{-(\omega_1+\omega_3)x}, \tag{14}$$

where

$$\begin{cases}\omega_1=\dfrac{\psi_{SR,s}}{a_2\rho_s\tilde{\beta}_{SR}},\quad \omega_2=\dfrac{\psi_{SD,s}}{a_2\rho_s\tilde{\beta}_{SD}},\quad \omega_3=\dfrac{\psi_{RD,r}}{b_2\rho_r\tilde{\beta}_{RD}},\\ \varphi_1=\dfrac{a_2\psi_{RD,r}\rho_s\tilde{\beta}_{SD}}{a_2\psi_{RD,r}\rho_s\tilde{\beta}_{SD}-b_2\psi_{SD,s}\rho_r\tilde{\beta}_{RD}},\\ \varphi_2=\dfrac{b_2\psi_{SD,s}\rho_r\tilde{\beta}_{RD}}{a_2\psi_{RD,r}\rho_s\tilde{\beta}_{SD}-b_2\psi_{SD,s}\rho_r\tilde{\beta}_{RD}}.\end{cases}$$

Proof: By definition, $\overline{F}_{\gamma_2}$ denotes the CCDF of γ_2 and can be calculated as follows:

$$\begin{aligned}&\overline{F}_{\gamma_2}(x)\\&=\Pr\left\{\frac{\tilde{\lambda}_{SR}a_2\rho_s}{\psi_{SR,s}}>x,\frac{\tilde{\lambda}_{SD}a_2\rho_s}{\psi_{SD,s}}+\frac{\tilde{\lambda}_{RD}b_2\rho_r}{\psi_{RD,r}}>x\right\}\\&=\Pr\left\{\tilde{\lambda}_{SR}>\frac{\psi_{SR,s}x}{a_2\rho_s}\right\}\cdot\Pr\left\{\frac{\tilde{\lambda}_{SD}a_2\rho_s}{\psi_{SD,s}}+\frac{\tilde{\lambda}_{RD}b_2\rho_r}{\psi_{RD,r}}>x\right\}\\&=e^{-\frac{\psi_{SR,s}x}{a_2\rho_s\tilde{\beta}_{SR}}}\cdot\left\{1-\int_0^{\frac{\psi_{SD,s}x}{a_2\rho_s}}\int_0^{\frac{(x-\frac{ua_2\rho_s}{\psi_{SD,s}})\psi_{RD,r}}{b_2\rho_r}}\frac{1}{\tilde{\beta}_{RD}}e^{-\frac{v}{\tilde{\beta}_{RD}}}\right.\\&\qquad\left.\cdot\frac{1}{\tilde{\beta}_{SD}}e^{-\frac{u}{\tilde{\beta}_{SD}}}dvdu\right\}\\&=\varphi_1e^{-(\omega_1+\omega_2)x}-\varphi_2e^{-(\omega_1+\omega_3)x}.\end{aligned} \tag{15}$$

Similar to (11), (14) can be obtained from (15), and the proof is completed. ■

Base on **Theorem 1**, using $\int_0^\infty\frac{1}{2}\log_2(1+x)f_\gamma(x)dx=\frac{1}{2\ln 2}\int_0^\infty\frac{1-F_\gamma(x)}{1+x}dx$, the ergodic achievable rate of s_1 can be given by

$$\begin{aligned}C_1&=\int_0^\infty\frac{1}{2}\log_2(1+x)f_{\gamma_1}(x)dx\\&=\frac{1}{2\ln 2}\int_0^\infty\frac{1-F_{\gamma_1}(x)}{1+x}dx\\&=\frac{1}{2\ln 2}\int_0^{\frac{a_1}{a_2}}\frac{1}{1+x}e^{-\left(\frac{\psi_{SR,s}\Omega(x)}{\tilde{\beta}_{SR}}+\frac{\psi_{SD,s}\Omega(\eta)}{\tilde{\beta}_{SD}}\right)}dx.\end{aligned} \tag{16}$$

Similarly, based on **Theorem 2**, we can obtain the ergodic achievable rate of s_2 as follows:

$$\begin{aligned}C_2&=\frac{1}{2\ln 2}\int_0^\infty\frac{1-F_{\gamma_2}(x)}{1+x}dx\\&=\frac{1}{2\ln 2}\int_0^\infty\frac{1}{1+x}\left\{\varphi_1e^{-(\omega_1+\omega_2)x}-\varphi_2e^{-(\omega_1+\omega_3)x}\right\}dx\\&=-\frac{\varphi_1}{2\ln 2}e^{\omega_1+\omega_2}Ei(-\omega_1-\omega_2)\\&\quad+\frac{\varphi_2}{2\ln 2}e^{\omega_1+\omega_3}Ei(-\omega_1-\omega_3),\end{aligned} \tag{17}$$

where we use $\int_0^\infty\frac{e^{-mx}}{1+x}dx=-e^mEi(-m)$ [35, eq. (8.212.5)], and $Ei(\cdot)$ denotes the exponential integral function [35, eq. (8.211.1)].

Finally, based on (16) and (17), the ergodic sum rate of our proposed scheme is obtained as

$$\begin{aligned} C_{sum} &= C_1 + C_2 \\ &= \frac{1}{2\ln 2}\int_0^{\frac{a_1}{a_2}} \frac{1}{1+x} e^{-\left(\frac{\psi_{SR,s}\Omega(x)}{\bar{\beta}_{SR}}+\frac{\psi_{SD,s}\Omega(\eta)}{\bar{\beta}_{SD}}\right)} dx \\ &\quad - \frac{\varphi_1}{2\ln 2} e^{\omega_1+\omega_2}\mathrm{Ei}\left(-\omega_1-\omega_2\right) \\ &\quad + \frac{\varphi_2}{2\ln 2} e^{\omega_1+\omega_3}\mathrm{Ei}(-\omega_1-\omega_3). \end{aligned} \tag{18}$$

B. OUTAGE PROBABILITY AND THROUGHPUT ANALYSIS

Outage probability denotes the probability of an event that the achievable rate is less than the predefined one, which is a good metric for quality of service (QoS) in the communication system design [36]. The outage probability is a decisive factor of the system throughput [37]– [39], the system throughput evaluates the average achieved rate where the symbols are successfully transmitted from the source to the destination. Thus the analysis of system throughput of our proposed CONOMA-TPSC scheme is practically significant since it characterize the average amount of messages which successfully transmitted in each communication.

Let R_1 and R_2 denote the target rates of s_1 and s_2, respectively. According to the NOMA protocol, the outage events of s_1 occur when $\frac{1}{2}\log_2(1+\gamma_1) < R_1$. Therefore, the outage probability of s_1 can be expressed as

$$\begin{aligned} P_{s_1} &= \Pr\{\gamma_1 < \phi_1\} = 1 - \Pr\{\gamma_1 > \phi_1\} \\ &= 1 - \Pr\left\{\gamma_1^R > \phi_1, \gamma_1^D > \phi_1\right\}, \end{aligned} \tag{19}$$

where $\phi_1 = 2^{2R_1} - 1$.

The following theorem provides the outage probability of s_1 for the proposed system.

Theorem 3: The closed-form expression for the outage probability of s_1 is given by

$$P_{s_1} = 1 - e^{-\left(\frac{\psi_{SR,s}\Omega(\phi_1)}{\bar{\beta}_{SR}}+\frac{\psi_{SD,s}\Omega(\varepsilon)}{\bar{\beta}_{SD}}\right)}, \tag{20}$$

where $\Omega(\theta) = \frac{\theta}{(a_1-\theta a_2)\rho_s}$ for $\theta \in \{\phi_1, \varepsilon\}$, $\varepsilon = \phi_1 - \frac{b_1}{b_2}$. Note (20) is derived by assuming the condition $a_1 > a_2\phi_1$ is satisfied.

Proof: Define $\overline{P}_{s_1}$ as the complementary outage probability of our proposed scheme, and using (8) we can obtain $\overline{P}_{s_1}$ as follows:

$$\begin{aligned} \overline{P}_{s_1} &= \Pr\left\{\gamma_1^R > \phi_1, \gamma_1^D > \phi_1\right\} \\ &= \Pr\left\{\frac{\tilde{\lambda}_{SR}a_1\rho_s}{\tilde{\lambda}_{SR}a_2\rho_s + \psi_{SR,s}} > \phi_1, \frac{\tilde{\lambda}_{SD}a_1\rho_s}{\tilde{\lambda}_{SD}a_2\rho_s + \psi_{SD,s}} \right. \\ &\quad \left. + \frac{\tilde{\lambda}_{RD}b_1\rho_r}{\tilde{\lambda}_{RD}b_2\rho_r + \psi_{RD,r}} > \phi_1\right\} \\ &\overset{(b)}{=} \Pr\left\{\frac{\tilde{\lambda}_{SR}a_1\rho_s}{\tilde{\lambda}_{SR}a_2\rho_s + \psi_{SR,s}} > \phi_1, \right. \\ &\quad \left. \frac{\tilde{\lambda}_{SD}a_1\rho_s}{\tilde{\lambda}_{SD}a_2\rho_s + \psi_{SD,s}} + \frac{b_1}{b_2} > \phi_1\right\} \\ &= \Pr\left\{\tilde{\lambda}_{SR} > \frac{\psi_{SR,s}\phi_1}{a_1\rho_s - xa_2\rho_s}, \tilde{\lambda}_{SD} > \frac{\psi_{SD,s}\varepsilon}{a_1\rho_s - \varepsilon a_2\rho_s}\right\} \\ &= e^{-\left(\frac{\psi_{SR,s}\Omega(\phi_1)}{\bar{\beta}_{SR}}+\frac{\psi_{SD,s}\Omega(\varepsilon)}{\bar{\beta}_{SD}}\right)}, \end{aligned} \tag{21}$$

where (b) follows from the approximation mentioned above. Substituting (21) into (19), (20) can be obtained and the proof is completed. ■

Similarly, the outage events at s_2 occur when $\frac{1}{2}\log_2(1+\gamma_2) < R_2$. The outage probability at s_2 can be expressed as

$$\begin{aligned} P_{s_2} &= 1 - \Pr\{\gamma_2 > \phi_2\} \\ &= 1 - \Pr\left\{\gamma_2^R > \phi_2, \gamma_2^D > \phi_2\right\}, \end{aligned} \tag{22}$$

where $\phi_2 = 2^{2R_2} - 1$.

The following theorem provides the outage probability of s_2 for our proposed scheme.

Theorem 4: The closed-form expression for the outage probability of s_2 is given by

$$P_{s_2} = 1 - \left(\varphi_1 e^{-(\omega_1+\omega_2)\phi_2} - \varphi_2 e^{-(\omega_1+\omega_3)\phi_2}\right). \tag{23}$$

Proof: Define $\overline{P}_{s_2}$ as the complementary outage probability of our proposed scheme, using (9), $\overline{P}_{s_2}$ can be expressed as follows:

$$\begin{aligned} \overline{P}_{s_2} &= \Pr\left\{\frac{\tilde{\lambda}_{SR}a_2\rho_s}{\psi_{SR,s}} > \phi_2, \frac{\tilde{\lambda}_{SD}a_2\rho_s}{\psi_{SD,s}} + \frac{\tilde{\lambda}_{RD}b_2\rho_r}{\psi_{RD,r}} > \phi_2\right\} \\ &= \Pr\left\{\tilde{\lambda}_{SR} > \frac{\psi_{SR,s}\phi_2}{a_2\rho_s}\right\} \\ &\quad \cdot \Pr\left\{\frac{\tilde{\lambda}_{SD}a_2\rho_s}{\psi_{SD,s}} + \frac{\tilde{\lambda}_{RD}b_2\rho_r}{\psi_{RD,r}} > \phi_2\right\} \\ &= \varphi_1 e^{-(\omega_1+\omega_2)\phi_2} - \varphi_2 e^{-(\omega_1+\omega_3)\phi_2}. \end{aligned} \tag{24}$$

Combing (22) and (24), (23) can be obtained and the proof is completed. ■

Based on **Theorem 3** and **Theorem 4**, the outage probability of the CRS-NOMA system can be expressed as follows:

$$\begin{aligned} P_{out} &= P_{s_1} + P_{s_2} - P_{s_1}\cdot P_{s_2} \\ &= 1 - e^{-\frac{\psi_{SR,s}\Omega(\phi_1)}{\bar{\beta}_{SR}}-\frac{\psi_{SD,s}\Omega(\varepsilon)}{\bar{\beta}_{SD}}} \\ &\quad \cdot \left(\varphi_1 e^{-(\omega_1+\omega_2)\phi_2} - \varphi_2 e^{-(\omega_1+\omega_3)\phi_2}\right). \end{aligned} \tag{25}$$

The source and the relay transmit information at constant rates R_1 and R_2, which is subjected to the effect of the outage probability due to the Rayleigh fading channels. The system throughput is defined as the product of the transmission rate and the successful communication probability. In this paper, we focus on the throughput for the whole system, thus the

system throughput of our proposed CONOMA-TPSC scheme can be expressed as follows:

$$\begin{aligned} R^{sum} &= (R_1 + R_2)(1 - P_{out}) \\ &= (R_1 + R_2)e^{-\frac{\psi_{SR,s}\Omega(\phi_1)}{\bar{\rho}_{SR}} - \frac{\psi_{SD,s}\Omega(\varepsilon)}{\bar{\rho}_{SD}}} \\ &\quad \cdot \left(\varphi_1 e^{-(\omega_1+\omega_2)\phi_2} - \varphi_2 e^{-(\omega_1+\omega_3)\phi_2}\right). \end{aligned} \quad (26)$$

The term $1 - P_{out}$ in (26) represents the successful transmission from the source to the destination of the proposed CONOMA-TPSC system.

In next section, we will apply numerical simulations to examine the ergodic sum rate, outage probability, and system throughput performance.

Remark 1 (Complexity Analysis): In our proposed CONOMA-TPSC scheme, the relay decodes the two symbols with SIC and forwards the two symbols with a new superposition coding , and the MRC will be employed in the destination to detect the symbols. According to the above analysis, the computational and application complexity of CONOMA-TPSC scheme is higher since we employ superposition coding and MRC at the relay and destination, respectively. The NCRS-NOMA [28] scheme comes second due to that the destination jointly decodes the signals with MRC and the CRS-NOMA [27] scheme gains the lowest complexity. Although complexity of our proposed CONOMA-TPSC scheme is higher than the NCRS-NOMA and CRS-NOMA schemes, the CONOMA-TPSC scheme achieves significant gains over NCRS-NOMA and CRS-NOMA, which will be verified in next Section.

Remark 2 (Signaling Overhead Analysis): There are several sources of signaling overhead in NOMA. For example, to obtain the CSI from different receivers. The signaling overhead caused by the CSI feedback of our proposed NCRS-NOMA scheme is equivalent to the NCRS-NOMA and CRS-NOMA schemes because of the fact that transmission channel of the three schemes are assumed to be the same. Another important source of signaling overhead in NOMA is the encoding and decoding of superposition code and SIC [6]. The superposition coding is employed both at the source and the relay in the proposed NCRS-NOMA scheme, however, only the source employs superposition coding in the NCRS-NOMA and CRS-NOMA schemes. Therefore, the CONOMA-TPSC scheme causes little higher signaling overhead than the schemes in [27] and [28].

IV. NUMERICAL RESULTS

In this section, we provide numerical results to examine the performance of our proposed CONOMA-TPSC scheme in terms of the ergodic sum rate, outage probability, and system throughput. The NCRS-NOMA and CRS-NOMA schemes in [27] and [28] are shown for comparison under perfect CSI (i.e., $\kappa = 0$ in this paper). Furthermore, Monte Carlo simulations are employed to verify the analytical expressions given in Section III. Comparisons are made with the recently proposed CRS-NOMA [27] and NCRS-NOMA [28] schemes in two considered system setups: $\beta_{SR} = \beta_{RD} = 10$ (case 1); $\beta_{SR} = 5$, $\beta_{RD} = 10$ (case 2) with $\beta_{SD} = 5$, $a_1 = 0.9$, and $a_2 = 0.1$. Meanwhile, we set $\sigma_{e_i}^2 = 1$ ($i \in SR, RD, SD$) in the following simulations. In this section, we assume that the source and relay have different transmit power, which is a widely adopted assumption in relay systems (e.g., [40], [41]) and in the context of NOMA systems (e.g., [20], [22]).

Fig. 2 and Fig. 3 plot the ergodic sum rate versus the transmission SNR at the source (i.e. ρ_s) and the relay (i.e. ρ_r) with $b_1 = 0.7$, $b_2 = 0.3$, and $\kappa = 0$, respectively. In Fig. 2, we set the transmission SNR at relay $\rho_r = 10$ dB in case 1 and case 2. The solid and dashed curves represent the sum rates in case 1 and case 2, respectively. In these figures, we can observe that the simulation and analytical results match well for the whole range of ρ_s, which validates the analytical expression of the ergodic sum rate in (18).

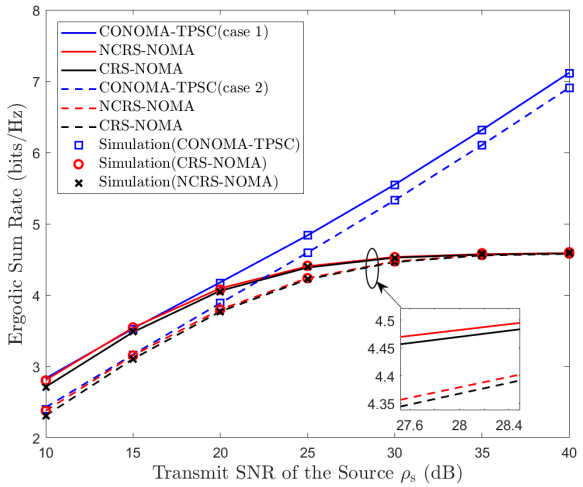

FIGURE 2. The ergodic sum rate achieved by the CONOMA-TPSC, NCRS-NOMA, and CRS-NOMA schemes versus the transmit SNR ρ_S with $b_1 = 0.7$, $b_2 = 0.3$, $\kappa = 0$, and $\rho_r = 10$ dB.

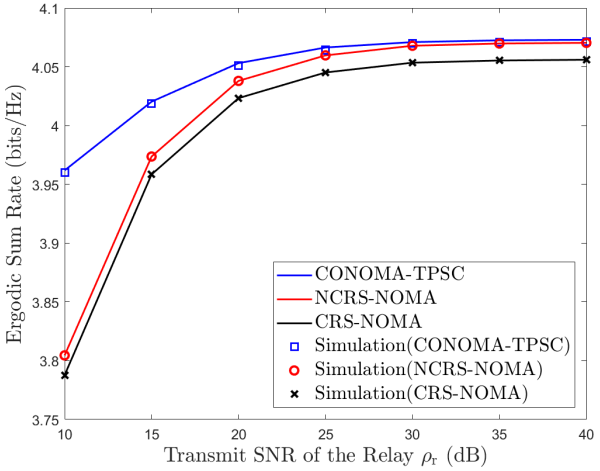

FIGURE 3. The ergodic sum rate achieved by the CONOMA-TPSC, NCRS-NOMA, and CRS-NOMA schemes versus the transmit SNR ρ_r with $b_1 = 0.7$, $b_2 = 0.3$, $\kappa = 0$, and $\rho_S = 20$ dB.

From Fig. 2, we can see that our proposed scheme outperforms the two schemes in [27] and [28] for a large transmit SNR range. From this figure, we also observe that, as the transmit SNR of the source (i.e., ρ_s) increases for a fixed transmit SNR of the relay (i.e., ρ_r), the achieved ergodic sum rate by our proposed CONOMA-TPSC scheme continuously increases, while those achieved by the NCRS-NOMA and CRS-NOMA schemes approach to a ceiling. The reasons are detailed as below. For the CRS-NOMA scheme proposed in [27], this is due to the fact that the SINR of s_1 given in (5) (in [27]) is interference-limited and it only approaches to a constant as ρ_s increases, while the SINR of s_2 is limited by the fixed ρ_r (since the direct transmission of s_2 from the source to the destinatsion is not utilized in [27], which is confirmed by [27, eq. (7)]). For the NCRS-NOMA scheme proposed in [28], the reason is similar to that of the CRS-NOMA scheme proposed in [27]. We note that the direct transmission of s_2 from the source to the destination is used. The received signals from the source and relay for decoding s_2 are combined by using MRC in [28]. However, this combining is conducted before SIC, which leads to the fact that the SINR of s_2 is still interference-limited as ρ_s increases. This is confirmed by [28, eq. (10)]. For our proposed CONOMA-TPSC scheme, this is due to the fact that the achievable rate C_2 is not interference-limited and can continuously increase as ρ_s (i.e., P_s) increases, which can be confirmed by our equations (4), (7), and (9). Intuitively, this is achieved by combining the received signals from the source and relay for decoding s_2 by using MRC after SIC, which leads to the fact that s_2 is not interference-limited and its corresponding SNR continuously increases as ρ_s increases.

In Fig. 3, we plot the ergodic sum rate versus the transmit SNR of the relay ρ_r with a fixed transmit SNR of the source $\rho_s = 20$ dB. From this figure, we can observe that our proposed CONOMA-TPSC scheme obtains significant advantages over the NCRS-NOMA and CRS-NOMA schemes when $\rho_s \neq \rho_r$. We also observe that the ergodic sum rates of these schemes converge to some specific ceilings in the high regime of ρ_r, which is due to the fact that ρ_s is the dominant impact factor on the performance of these schemes when ρ_r is high. From Fig. 2 and Fig. 3, we can see that our proposed CONOMA-TPSC scheme can still outperform the NCRS-NOMA and CRS-NOMA schemes in the special case of $\rho_s = \rho_r$, although the performance gain is lower than that achieved in the case with $\rho_s \neq \rho_r$.

In Fig. 4, we plot the outage probability versus the transmit SNR at the source. We set $b_1 = 0.7$, $b_2 = 0.3$, and $R_1 = R_2 = 1$. We can find that the performance of the outage probability is getting better with the increases of the transmit power of the source in all these schemes, and our proposed scheme achieves the best performance, especially when the transmit power of the source is large since we employ superposition coding at R-D phase.

From Fig. 2 and Fig. 4, we can observe that the NCRS-NOMA scheme gains little advantage over the CRS-NOMA scheme in this situation. We can also find that

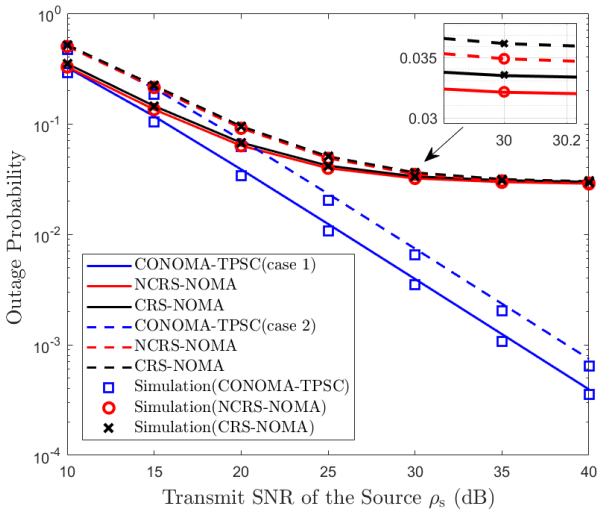

FIGURE 4. The outage probability achieved by the CONOMA-TPSC, NCRS-NOMA, and CRS-NOMA schemes versus the transmit SNR ρ_S with $b_1 = 0.7$, $b_2 = 0.3$, $\rho_r = 10$ dB, $\kappa = 0$, and $R_1 = R_2 = 1$.

our proposed scheme significantly outperforms the existing CRS-NOMA schemes, since we employ the superposition coding at the relay.

In Fig. 5, we plot the system throughput versus the transmission SNR at the source for CONOMA-TPSC, NCRS-NOMA, and CRS-NOMA schemes. We set the target rates as $R_1 = 0.8$ and $R_2 = 1.2$. It can be easily seen that the proposed CONOMA-TPSC scheme outperforms the NCRS-NOMA, and CRS-NOMA schemes in terms of throughput performance. It can also be observed that the system throughput converges to a constant for the CONOMA-TPSC, NCRS-NOMA, and CRS-NOMA schemes with the increase of ρ_s. Furthermore, the throughput of the CONOMA-TPSC tends to the sum value of R_1 and R_2, and the throughput ceilings of the NCRS-NOMA

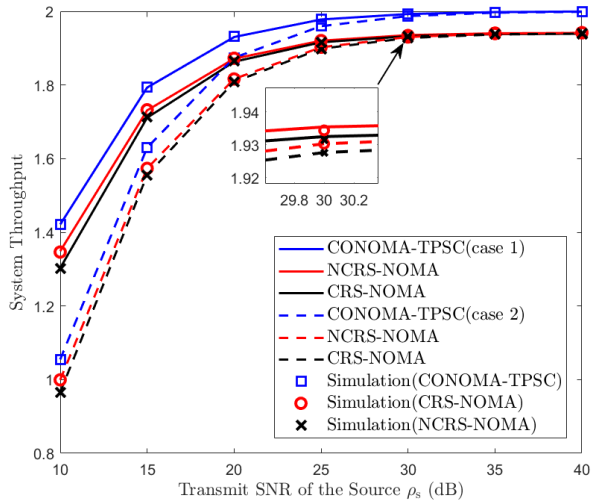

FIGURE 5. The system throughput achieved by the CONOMA-TPSC, NCRS-NOMA, and CRS-NOMA schemes versus the transmit SNR ρ_S with $b_1 = 0.7$, $b_2 = 0.3$, $\rho_r = 10$ dB, $\kappa = 0$, and $R_1 = R_2 = 1$.

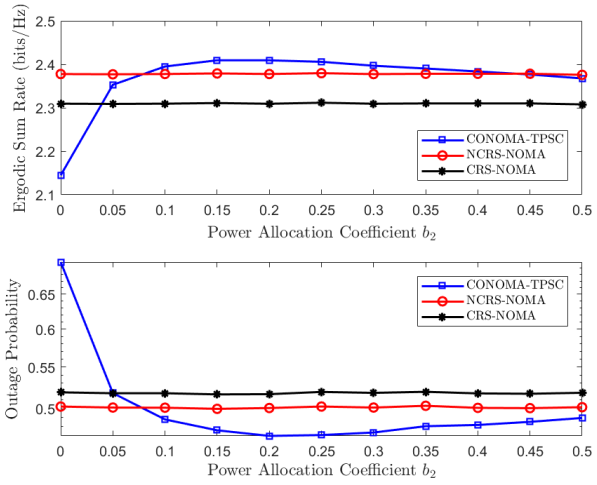

FIGURE 6. The ergodic sum rate and outage probability versus the power allocation coefficient b_2 with $\rho_S = 20$ dB, $\rho_r = 20$ dB, $\kappa = 0$ and $R_1 = R_2 = 1$.

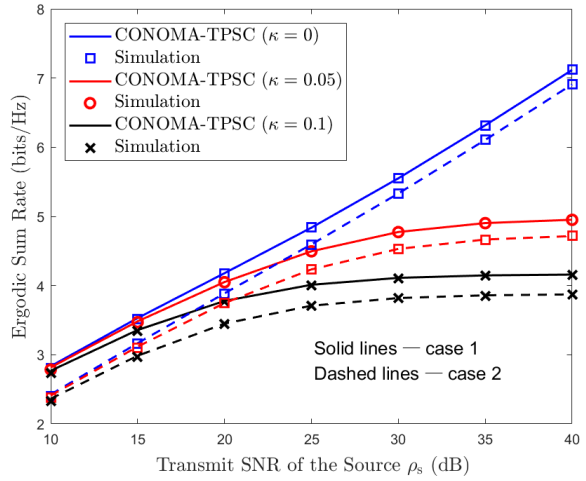

FIGURE 7. The ergodic sum rate achieved by the CONOMA-TPSC scheme versus the transmit SNR ρ_S with different values of κ when $b_1 = 0.7$, $b_2 = 0.3$, and $\rho_r = 10$ dB.

and CRS-NOMA schemes are lower than that of our proposed scheme. The reason is that in the high transmission SNR region, the successful transmission probability $1 - P_{out}$ is small and has little effect on the system throughput, and the throughput only depends on the fixed target transmission rates R_1 and R_2. In addition, we can observe that the outage probabilities of the NCRS-NOMA and CRS-NOMA schemes tend to specific constants with the increase of ρ_s in Fig. 4, thereby making the system throughput slightly lower than the sum value of R_1 and R_2.

In Fig. 6, we investigate the influence of power allocation coefficient b_2 ($b_1 = 1 - b_2$) over the performance of ergodic sum rate and outage probability for our proposed CONOMA-TPSC scheme. In the top sub-figure, we show the impact of the power allocation over the performance of ergodic sum rate, while in the bottom sub-figure, the impact

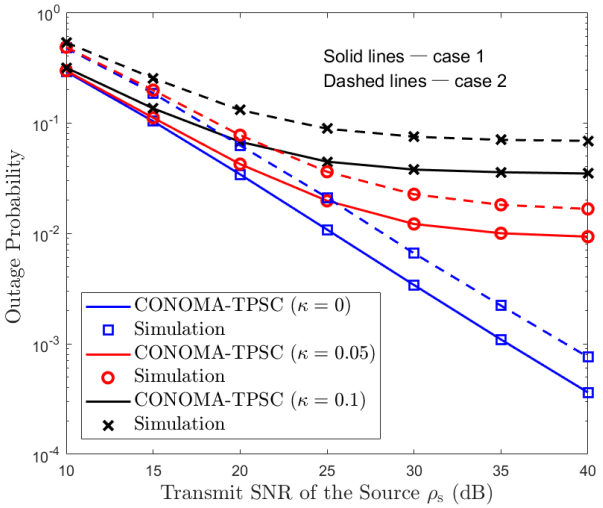

FIGURE 8. The outage probability achieved by the CONOMA-TPSC scheme versus the transmit SNR ρ_S with different values of κ when $b_1 = 0.7$, $b_2 = 0.3$, and $\rho_r = 10$ dB.

on outage probability with $R_1 = R_2 = 1$ is provided. It is obvious that a good power allocation coefficients based on the balance of the ergodic sum rate and outage probability can achieve a remarkable gain in the NCRS-NOMA scheme compared to the NCRS-NOMA and CRS-NOMA schemes.

In Fig. 7 and Fig. 8, we further examine the impact of the channel estimation error on the ergodic sum rate and outage probability. In this two figures, we can observe that the performance of the system performance in terms of the ergodic sum rate and outage probability becomes worse with the increase of κ, since a bigger κ indicates a severer imperfect impact.

V. CONCLUSION

In this paper, we proposed a cooperative NOMA relaying system CONOMA-TPSC and we derived the ergodic sum rate, outage probability, and system throughput to characterize the performance of our proposed scheme with imperfect CSI taken into account. The numerical results indicated that our proposed scheme achieved a remarkable gain over the existing schemes in [27] and [28]. It is noteworthy that power allocation coefficients are very important to the performance of CONOMA-TPSC. For future work, possible schemes that allow the source to transmit the signal in the second time slot with full-duplex decode-and-forward relay will be involved in order to make a further enhancement on the system performance, and new emerging technologies like Massive MIMO will be considered in our future works.

REFERENCES

[1] J. G. Andrews *et al.*, "What will 5G be?" *IEEE J. Sel. Areas Commun.*, vol. 32, no. 6, pp. 1065–1082, Jun. 2014.

[2] Z. Ding *et al.*, "Application of non-orthogonal multiple access in LTE and 5G networks," *IEEE Commun. Mag.*, vol. 55, no. 2, pp. 185–191, Feb. 2017.

[3] Z. Chen, Z. Ding, X. Dai, and R. Zhang, "An optimization perspective of the superiority of noma compared to conventional OMA," *IEEE Trans. Signal Process.*, vol. 65, no. 19, pp. 5191–5202, Oct. 2017.

[4] Y. Saito, Y. Kishiyama, A. Benjebbour, T. Nakamura, A. Li, and K. Higuchi, "Non-orthogonal multiple access (NOMA) for cellular future radio access," in *Proc. IEEE 77th Veh. Technol. Conf. (VTC Spring)*, Dresden, Germany, Jun. 2013, pp. 1–5.

[5] L. Dai, B. Wang, Y. Yuan, S. Han, C.-L. I, and Z. Wang, "Non-orthogonal multiple access for 5G: Solutions, challenges, opportunities, and future research trends," *IEEE Commun. Mag.*, vol. 53, no. 9, pp. 74–81, Sep. 2015.

[6] S. M. R. Islam, N. Avazov, O. A. Dobre, and K.-S. Kwak, "Power-domain non-orthogonal multiple access (NOMA) in 5G systems: Potentials and challenges," *IEEE Commun. Surveys Tuts.*, vol. 19, no. 2, pp. 721–742, 2nd Quart., 2017.

[7] H. Nikopour *et al.*, "SCMA for downlink multiple access of 5G wireless networks," in *Proc. IEEE Global Commun. Conf. (GLOBECOM)*, Austin, TX, USA, Dec. 2014, pp. 3940–3945.

[8] B. Ling, C. Dong, J. Dai, and J. Lin, "Multiple decision aided successive interference cancellation receiver for NOMA systems," *IEEE Wireless Commun. Lett.*, vol. 6, no. 4, pp. 498–501, Aug. 2017.

[9] F. R. Kschischang, B. J. Frey, and H.-A. Loeliger, "Factor graphs and the sum-product algorithm," *IEEE Trans. Inf. Theory*, vol. 47, no. 2, pp. 498–519, Feb. 2001.

[10] M. Moltafet, N. M. Yamchi, M. R. Javan, and P. Azmi, "Comparison study between PD-NOMA and SCMA," *IEEE Trans. Veh. Technol.*, vol. 67, no. 2, pp. 1830–1834, Feb. 2018.

[11] M. Moltafet, N. Mokari, M. R. Javan, H. Saeedi, and H. Pishro-Nik, "A new multiple access technique for 5G: Power domain sparse code multiple access (PSMA)," *IEEE Access*, vol. 6, pp. 747–759, 2018.

[12] Z. Ding, Z. Yang, P. Fan, and H. V. Poor, "On the performance of non-orthogonal multiple access in 5G systems with randomly deployed users," *IEEE Signal Process. Lett.*, vol. 21, no. 12, pp. 1501–1505, Dec. 2014.

[13] Y. Saito, A. Benjebbour, Y. Kishiyama, and T. Nakamura, "System-level performance of downlink non-orthogonal multiple access (NOMA) under various environments," in *Proc. IEEE 81st Veh. Technol. Conf. (VTC Spring)*, Glasgow, U.K., May 2015, pp. 1–5.

[14] M. F. Kader, M. B. Shahab, and S. Y. Shin, "Exploiting non-orthogonal multiple access in cooperative relay sharing," *IEEE Commun. Lett.*, vol. 21, no. 5, pp. 1159–1162, May 2017.

[15] J. Choi, "Non-orthogonal multiple access in downlink coordinated two-point systems," *IEEE Commun. Lett.*, vol. 18, no. 2, pp. 313–316, Feb. 2014.

[16] M. F. Kader, S. Y. Shin, and V. C. M. Leung, "Full-duplex non-orthogonal multiple access in cooperative relay sharing for 5G systems," *IEEE Trans. Veh. Technol.*, to be published.

[17] X. Yue, Y. Liu, S. Kang, A. Nallanathan, and Z. Ding, "Outage performance of full/half-duplex user relaying in NOMA systems," in *Proc. IEEE Int. Conf. Commun. (ICC)*, Paris, France, May 2017, pp. 1–6.

[18] Z. Ding, M. Peng, and H. V. Poor, "Cooperative non-orthogonal multiple access in 5G systems," *IEEE Commun. Lett.*, vol. 19, no. 8, pp. 1462–1465, Aug. 2015.

[19] J.-B. Kim and I.-H. Lee, "Non-orthogonal multiple access in coordinated direct and relay transmission," *IEEE Commun. Lett.*, vol. 19, no. 11, pp. 2037–2040, Nov. 2015.

[20] X. Liu, X. Wang, and Y. Liu, "Power allocation and performance analysis of the collaborative NOMA assisted relaying systems in 5G," *China Commun.*, vol. 14, no. 1, pp. 50–60, Jan. 2017.

[21] T. N. Do, D. B. da Costa, T. Q. Duong, and B. An, "Improving the performance of cell-edge users in NOMA systems using cooperative relaying," *IEEE Trans. Commun.*, vol. 66, no. 5, pp. 1883–1901, May 2018.

[22] L. Zhang, J. Liu, M. Xiao, G. Wu, Y.-C. Liang, and S. Li, "Performance analysis and optimization in downlink NOMA systems with cooperative full-duplex relaying," *IEEE J. Sel. Areas Commun.*, vol. 35, no. 10, pp. 2398–2412, Oct. 2017.

[23] M. Mohammadi, B. K. Chalise, H. A. Suraweera, C. Zhong, G. Zheng, and I. Krikidis, "Throughput analysis and optimization of wireless-powered multiple antenna full-duplex relay systems," *IEEE Trans. Commun.*, vol. 64, no. 4, pp. 1769–1785, Apr. 2016.

[24] Z. Ding, H. Dai, and H. V. Poor, "Relay selection for cooperative NOMA," *IEEE Wireless Commun. Lett.*, vol. 5, no. 4, pp. 416–419, Aug. 2016.

[25] D. Deng, L. Fan, X. Lei, W. Tan, and D. Xie, "Joint user and relay selection for cooperative NOMA networks," *IEEE Access*, vol. 5, pp. 20220–20227, 2017.

[26] P. Xu, Z. Yang, Z. Ding, and Z. Zhang, "Optimal relay selection schemes for cooperative NOMA," *IEEE Trans. Veh. Technol.*, to be published.

[27] J.-B. Kim and I.-H. Lee, "Capacity analysis of cooperative relaying systems using non-orthogonal multiple access," *IEEE Commun. Lett.*, vol. 19, no. 11, pp. 1949–1952, Nov. 2015.

[28] M. Xu, F. Ji, M. Wen, and W. Duan, "Novel receiver design for the cooperative relaying system with non-orthogonal multiple access," *IEEE Commun. Lett.*, vol. 20, no. 8, pp. 1679–1682, Aug. 2016.

[29] W. Duan, M. Wen, Z. Xiong, and M. H. Lee, "Two-stage power allocation for dual-hop relaying systems with non-orthogonal multiple access," *IEEE Access*, vol. 5, pp. 2254–2261, 2017.

[30] S. Yan, N. Yang, G. Geraci, R. Malaney, and J. Yuan, "Optimization of code rates in SISOME wiretap channels," *IEEE Trans. Wireless Commun.*, vol. 14, no. 11, pp. 6377–6388, Nov. 2015.

[31] N. Yang, S. Yan, J. Yuan, R. Malaney, R. Subramanian, and I. Land, "Artificial noise: Transmission optimization in multi-input single-output wiretap channels," *IEEE Trans. Commun.*, vol. 63, no. 5, pp. 1771–1783, May 2015.

[32] Y. Feng, S. Yan, Z. Yang, N. Yang, and W.-P. Zhu, "TAS-based incremental hybrid decode–amplify–forward relaying for physical layer security enhancement," *IEEE Trans. Commun.*, vol. 65, no. 9, pp. 3876–3891, Sep. 2017.

[33] J. Men, J. Ge, and C. Zhang, "Performance analysis for downlink relaying aided non-orthogonal multiple access networks with imperfect CSI over Nakagami-*m* fading," *IEEE Access*, vol. 5, pp. 998–1004, 2016.

[34] M. R. Bhatnagar, "On the capacity of decode-and-forward relaying over Rician fading channels," *IEEE Commun. Lett.*, vol. 17, no. 6, pp. 1100–1103, Jun. 2013.

[35] I. S. Gradshteyn and I. M. Ryzhik, *Table of Integrals, Series, and Products*, 7th ed. Orlando, FL, USA: Academic, 2007.

[36] H. Sun, Q. Wang, R. Q. Hu, and Y. Qian, "Outage probability study in a NOMA relay system," in *Proc. IEEE Wireless Commun. Netw. Conf. (WCNC)*, San Francisco, CA, USA, Mar. 2017, pp. 1–6.

[37] A. A. Nasir, X. Zhou, S. Durrani, and R. A. Kennedy, "Relaying protocols for wireless energy harvesting and information processing," *IEEE Trans. Wireless Commun.*, vol. 12, no. 7, pp. 3622–3636, Jul. 2013.

[38] Y. Feng, Z. Yang, and S. Yan, "Non-orthogonal multiple access and artificial-noise aided secure transmission in FD relay networks," in *Proc. IEEE Globecom Workshops (GC Wkshps)*, Singapore, Dec. 2017, pp. 1–6.

[39] X. Yue, Y. Liu, S. Kang, and A. Nallanathan, "Performance analysis of NOMA with fixed gain relaying over Nakagami-*m* fading channels," *IEEE Access*, vol. 5, pp. 5445–5454, 2017.

[40] Y. Yang, Q. Li, W.-K. Ma, J. Ge, and P. C. Ching, "Cooperative secure beamforming for AF relay networks with multiple eavesdroppers," *IEEE Signal Process. Lett.*, vol. 20, no. 1, pp. 35–38, Jan. 2013.

[41] Q. Li, Y. Yang, W. K. Ma, M. Lin, J. Ge, and J. Lin, "Robust cooperative beamforming and artificial noise design for physical-layer secrecy in AF multi-antenna multi-relay networks," *IEEE Trans. Signal Process.*, vol. 63, no. 1, pp. 206–220, Jan. 2015.

YINGYING ZHANG received the B.S. degree in electronic and information engineering from the Anhui University of Finance and Economics, Anhui, China, in 2016. She is currently pursuing the M.S. degree with the Nanjing University of Posts and Telecommunications, Nanjing, China. Her research interests include wireless communication networks, signal processing, non-orthogonal multiple access, and cooperative communications.

ZHEN YANG received the B.Eng. and M.Eng. degrees from the Nanjing University of Posts and Telecommunications, China, in 1983 and 1988, respectively, and the Ph.D. degree from Shanghai Jiao Tong University, China, in 1999, all in electrical engineering. He was a Lecturer with the Nanjing University of Posts and Telecommunications in 1983, where he was promoted to an Associate Professor in 1995 and then a Full Professor in 2000. He was a Visiting Scholar with Bremen University, Germany, from 1992 to 1993, and an Exchange Scholar with Maryland University, USA, in 2003. He has published over 200 papers in academic journals and conferences. His research interests include various aspects of signal processing and communication, such as communication systems and networks, cognitive radio, spectrum sensing, speech and audio processing, compressive sensing, and wireless communication. He serves a member of Editorial Board for several other journals, such as the *Chinese Journal of Electronics*, *China Communications*, and *Data Collection and Processing*. He was the Chair of Asian Pacific Communication Conference Steering Committee from 2013 to 2014. He also as the Vice Chairman and a fellow of the Chinese Institute of Communications, the Chairman of the Jiangsu Institute of Internets, and the Vice Director of the Editorial Board of The *Journal on Communications*.

YOUHONG FENG (S'16) received the B.S. and M.S. degrees in information engineering from Chang'an University, Xi'an, China, in 2003 and 2006, respectively. He is currently pursuing the Ph.D. degree with the Nanjing University of Posts and Telecommunications. From 2017 to 2018, he was a Visiting Student with The Australian National University, Canberra, Australia. He is currently an Associate Professor with the College of Physics and Electronic Information Engineering, Anhui Normal University. His current research interests focus on resource allocation of wireless communication networks, cooperative communications, energy-efficient communications, and physical layer security.

SHIHAO YAN (S'11–M'15) received the B.S. degree in communication engineering and the M.S. degree in communication and information systems from Shandong University, Jinan, China, in 2009 and 2012, respectively, and the Ph.D. degree in electrical engineering from the University of New South Wales, Sydney, Australia, in 2015. From 2015 to 2017, he was a Post-Doctoral Research Fellow with the Research School of Engineering, The Australian National University, Canberra, Australia. He is currently a Research Fellow with the School of Engineering, Macquarie University, Sydney, Australia. His current research interests are in the areas of wireless communications and statistical signal processing, including physical layer security, covert communications, and location spoofing detection.